Biosensors and Bioelectronics 55 (2014) 91–98

Contents lists available at ScienceDirect

Biosensors and Bioelectronics

journal homepage: www.elsevier.com/locate/bios

Colorimetric detection of DNA hybridization based on a dual platform of gold nanoparticles and graphene oxide

Jeevan Thavanathan [a], Nay Ming Huang [a,*], Kwai Lin Thong [b]

[a] Low Dimension Material Research Center, Department of Physics, Faculty of Science, University of Malaya, 50603 Kuala Lumpur, Malaysia
[b] Institute of Biological Sciences, Faculty of Science, University of Malaya, 50603 Kuala Lumpur, Malaysia

ARTICLE INFO

Article history:
Received 3 September 2013
Received in revised form
24 November 2013
Accepted 28 November 2013
Available online 10 December 2013

Keywords:
Colorimetric biosensor
Colorimetric detection
DNA hybridization
DNA probe
Gold nanoparticles
Graphene oxide

ABSTRACT

The unique property of gold nanoparticles (Au NP) to induce colour change and the versatility of graphene oxides (GO) in surface modification makes them ideal in the application of colorimetric biosensor. Thus we developed a label free optical method to detect DNA hybridization through a visually observed colour change. The Au NP is conjugated to a DNA probe and is allowed to hybridize with the DNA target to the GO thus causing a change in colour from pinkish-red to purplish blue. Spectrophometry analysis gave a wavelength shift of 22 nm with 1 μM of DNA target. Sensitivity testing using serially diluted DNA conjugated GO showed that the optimum detection was at 63 nM of DNA target with the limit at 8 nM. This proves the possibility for the detection of DNA hybridization through the use of dual nanoparticle system by visual observation.

1. Introduction

The recent interest in research and development of DNA biosensors was stimulated by innovations done in the utilization of nanoparticles as detection probes (Merkoçi, 2010). DNA biosensors are highly valued tools in several fields such as genetic analysis (Tothill, 2009), food safety (Sharma and Mutharasan, 2013), environmental protection (Farré and Barceló, 2003), forensic applications (Redshaw et al., 2007) and defence interest (Paddle, 1996). Hence numerous types and techniques of DNA biosensors based on colorimetry (Xiang et al., 2012b; Zheng et al., 2012), electrochemiluminescence (Gao et al., 2013; Lu et al., 2013), electrochemistry (Wang, 2002), fluorescence (Zhao et al., 2012), surface plasmon resonance spectroscopy (Eum et al., 2009; Tawa et al., 2005) and quartz crystal microbalance (Hao et al., 2011; Kleo et al., 2011) have been researched and developed for the detection of DNA. Colorimetric based DNA biosensor provides an accurate data in the detection of DNA hybridization in terms of high sensitivity in the range of nano molar concentration (Qi et al., 2009), low cost production (Xiang et al., 2012a), rapidity of result (Zhan et al., 2012), and finally its simplistic design in colour detection (Baptista et al., 2005). Colorimetric biosensor is a subset within the labelled optical biosensors in which the probes are mostly modified with either fluorescent tags (Tolley et al., 2003) or luminescence tags (Wood and Gruber, 1996) for the purpose of quantitative detection. The use of gold nanoparticles (Au NP) in optical biosensor (Zhan et al., 2012) gives a new detection angle approach in which results are visually observed without the use of any additional detection instruments, thus making such systems amenable for point of care testing through qualitative analysis.

Au NP has emerged as the choice in detection and identification of DNA in recent decade for colorimetric biosensor due to its chemical and physical properties (Zhou et al., 2009). The nano-optical properties of Au NP have been well illustrated by studies on surface plasmon band (SPB) (Lismont and Dreesen, 2012), surface-enhanced Raman scattering (SERS) (Yang et al., 2007), and Rayleigh resonance scattering (RRS) (He et al., 2005). The simple colour change from red to blue elicited by the aggregation of the Au NP due to the change in distance between particles provides a simple mechanism of manipulation in developing a biosensor. This phenomenon is explained through the change in its surface plasmon resonance (Huang and El-Sayed, 2010). It was also reported that the ability to immobilize single stranded DNA onto the surface of the Au NP provides a buffer against aggregation in high salt environment. Reversing the non-cross linking process through DNA hybridization forming double stranded DNA caused a change in colour of the Au NP solution (Sato et al., 2003). A second technique utilizing cross linking between two DNA probes immobilized onto Au NP through an unmodified complementary DNA target as a linker was reported

* Corresponding author. Tel.: +60 12 209 1008; fax: +60 37 967 4146.
E-mail addresses: jeevanmacho@yahoo.com (J. Thavanathan), huangnayming@gmail.com, huangnayming@um.edu.my (N.M. Huang), thongkl@um.edu.my (K.L. Thong).

0956-5663/$ - see front matter © 2013 Elsevier B.V. All rights reserved.
http://dx.doi.org/10.1016/j.bios.2013.11.072

(Baptista et al., 2005). With the introduction of the unmodified DNA target linker, an instantaneous colour change was observed within the Au NP conjugated DNA probe solution (Cao et al., 2005). This technique provided us a base reference in the development of an experimental system for the detection of DNA hybridization which would be discussed in this paper.

By utilizing the cross-linking method as a guideline, we designed a system consisting of two different nanoparticles immobilized with complementary DNA probe and target. The purpose was to measure its effectiveness in inducing a colour change through DNA hybridization. The primary nanoparticle chosen to be immobilized with the DNA probe was Au NP. Graphene oxide (GO) was chosen as the secondary nanoparticle to be immobilized with the DNA target. GO is used as the secondary nano-component because it is of a single layer atomic thickness sheet which provides a large surface area sufficient for the immobilization of higher concentration of DNA on a single plane, thus providing a larger hybridization area and higher sensitivity (Loh et al., 2010). The flat surface of the GO is littered with numerous functional groups such as carboxylic and hydroxyl groups which present an easy route for DNA immobilization (Wu et al., 2011). The appearance of GO sheets being transparent avoids interference in the colour change ability of the colorimetric system. It also uses 50% less Au NP when compared to conventional optical based Au NP biosensors. Thus this study was to design and produce a basic working model of a dual nanoparticle colorimetric system in the detection of DNA hybridization utilizing a pair of complementary modified DNA strands.

2. Materials and methods

2.1. Chemicals and instruments

Hydrogen tetrachloroaurate ($HAuCl_4$), trisodium citrate (Na_3-$C_6H_5O_7$), and graphite flakes were purchased from Acros Organics (USA) while 1-Ethyl-3-(3-dimethylaminopropyl) carobodiimide (EDC), N-hydroxy sulfosuccinimide (Sulfo-NHS), dithiothreitol (DTT), N,N-dimethylformamide (DMF), potassium permanganate ($KMnO_4$), sulphuric acid (H_2SO_4), and phosphoric acid (H_3PO_4) were bought from Sigma-Aldrich (USA). Conjugation of the modified DNA to the Au NP through purification and activation of the thiol linkages was done using the NAP-10 sephadex columns, (G-25, GE Healthcare). The preparation of Au NP conjugated DNA probe (Au NP-DNA) and GO conjugated DNA target (GO-DNA) was carried out with a high speed centrifuge (MIKRO 220R, HETTICH). Wavelength scans on the

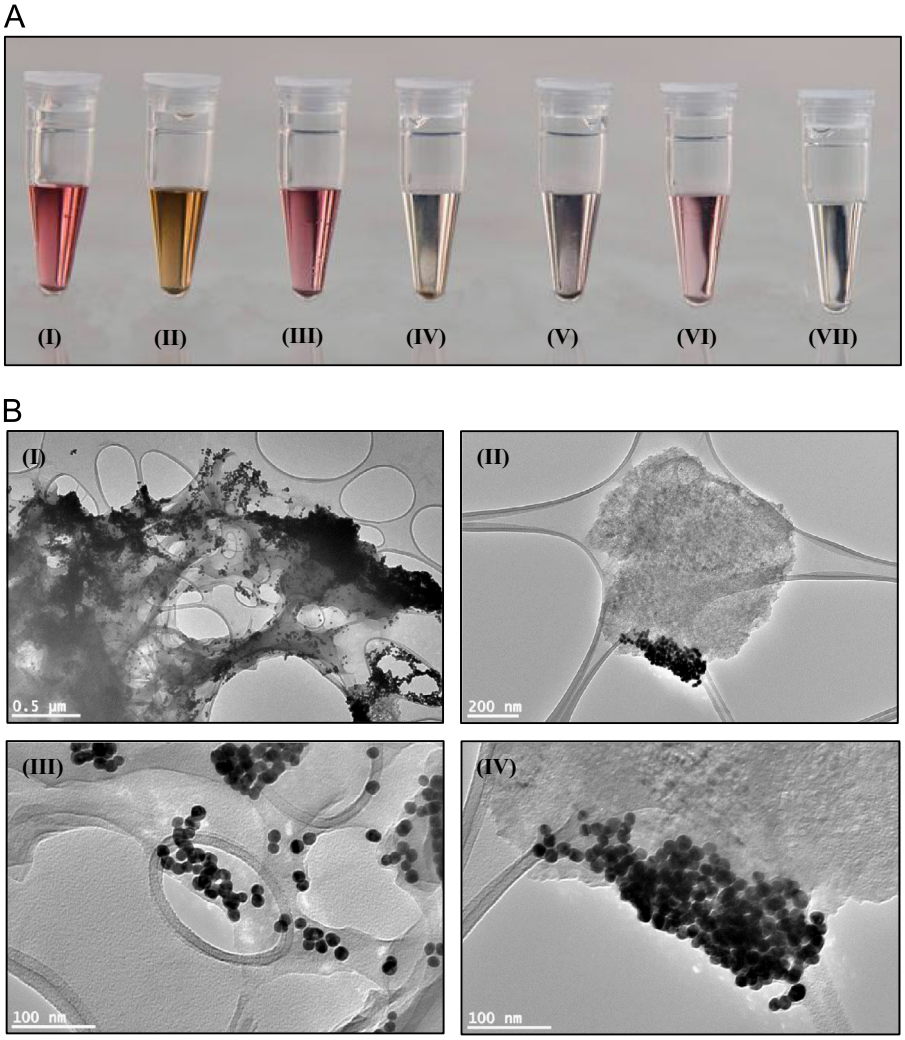

Fig. 1. (A) Visual observation of (I) ruby red Au NP solution, (II) golden-brown GO solution, (III) pinkish-red solution of Au NP-DNA, (IV) light brown solution of GO-DNA, (V) purplish-blue solution of the biosensor consisting hybridized Au NP-DNA and GO-DNA, (VI) pinkish-red solution of negative control consisting Au NP-DNA and Non-specific GO-DNA and (VII) transparent light brown solution of negative control with the mixture of GO-DNA and Non-specific probe DNA, (B) HRTEM images of (I) high conc. sample of the hybridized biosensor, (II) and (III) low conc. samples of the Au NP-DNA hybridizing on the edge of the GO-DNA sheets with no free floating Au NP-DNA observed. (IV) Higher magnification image of HRTEM image (II). (For interpretation of the references to color in this figure legend, the reader is referred to the web version of this article.)

detection of DNA hybridization and the individual platforms of Au NP-DNA and GO-DNA were performed using a UV-visible spectrophotometer (EVO300-PC, Thermo Scientific). Microscopic imaging of the Au NP conjugated DNA probe was done utilizing a high resolution transmission microscope (HRTEM, JEM 2100F, JEOL) by drop casting 0.5 μl of sample on a lacy carbon coated copper grid. A field-emission scanning electron microscope (FESSEM, JSM 7600F, JEOL) was used for imaging of the GO solution by drop casting 1 μl of sample onto a silicon oxide coated silicon wafer. Visual observation of the biosensor under colour changing condition was captured with the use of a professional grade full frame digital single-lens reflex camera (D4, Nikon).

2.2. Probe and target DNAs

The synthetic-DNAs used in the biosensor were categorized into two types, complementary and non-complementary sequences. The oligonucleotide sequences were designed in-house to detect the 148 bp *inv*A gene of the bacteria *Salmonella enterica*. Two sequences complementary to the *inv*A gene with the length of 22 bp were chosen to be the DNA probe and target. The DNA probe was subjected to modification of thiol linkages to its 5′ end while the DNA target was subjected to amino linkages on it 5′ end. The complementary sequences are as listed:-:

- DNA probe: 5′HS-AGG ATG TTA TTC GCA AAG GGA T-3′.
- DNA target: 5′H_2N-ATC CCT TTG CGA ATA ACA TCC T-3′.

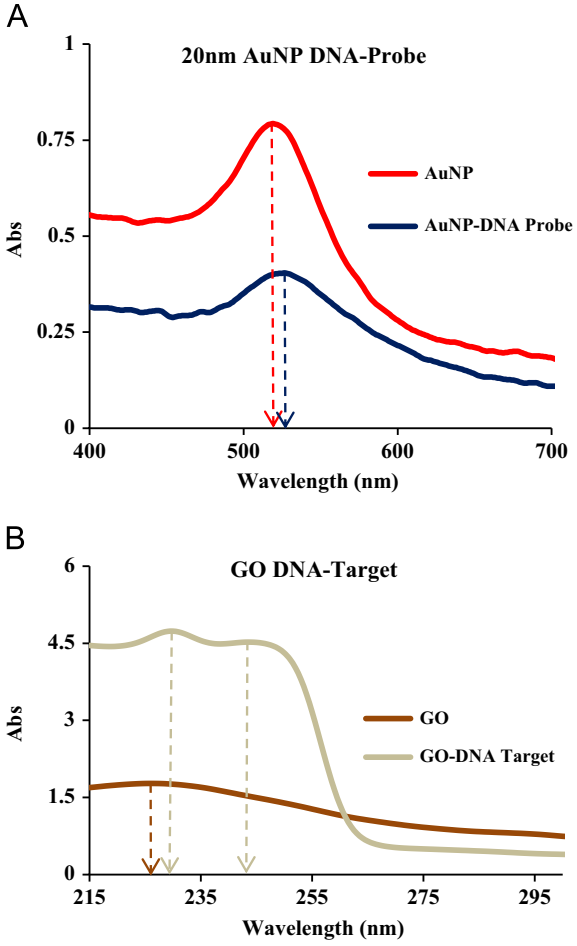

Fig. 2. (A) Wavelength scan of 20 nm Au NP with Au NP-DNA (B) Wavelength scan of GO particles and GO-DNA.

The non-complementary sequences were designed based on the *hem*M gene of the bacteria *Vibrio cholera* (Lalitha et al., 2008). Two sequences of 20 bp which were not complementary to both the *inv*A gene DNA probe and target were chosen to function as the negative samples in the selectivity experiments. The non-complementary target DNA sequence was modified with amino linkages while the non-complementary probe DNA sequence was not modified. The non-complementary sequences are as listed:-

- Non-complementary probe: 5′-CTC ACT GCG TTT AAG CAA TT-3′.
- Non-complementary target: 5′H_2N-AAT TGC TTA AAC GCA GTG AG-3′.

All the oligonucleotide sequences were purchased from Bioneer Corporation (South Korea).

2.3. Synthesis of Au NP and GO

The production of 20 nm Au NP was done through the citrate reduction method which was developed by Turkevich in 1951 and further improved by Frens in 1973 (Nguyen et al., 2011). The 20 nm Au NP was prepared according to standard procedure (Wu et al., 2012). The synthesis of GO was done using the improved phosphoric acid protocol, which yielded particles of high quantity and rich in oxidative functional groups (Marcano et al., 2010). The final GO mixture was centrifuged at 4000 rpm to remove the acidic impurities and subjected to prolong sonication to separate the layers of the sheets further. Sonication was also performed to break the sheets into smaller particles to provide a higher surface area to size ratio which would assist in the later immobilization of DNA onto it. Wavelength scanning through spectrophotometry was done to confirm the production of the nanoparticles while HRTEM and FESEM imaging was used to determine the size and shape.

2.4. DNA immobilization

The probe and target DNAs were separately immobilized onto their respective nanoparticles through their specific modification on the 5′ end of each strand. The conjugation of the DNA probe to the Au NP was done through thiol linkages (Kim et al., 2006). Absorbance was measured at 260 nm to determine the concentration of activated thiol modified DNA probe in the plastic microfuge tubes, which would subsequently be used to conjugate with the Au NP. The activated thiol modified DNA probe was added into 1 ml of pure Au NP solution and wrapped in foil to facilitate conjugation for 16 h. The Au NP-DNA solution was centrifuged at 13,000 rpm for 30 min to remove excess unconjugated DNA and Au NP. The pellet was dispersed in 0.3 M NaCl of 0.01 M phosphate buffer at pH 7.0. The DNA target sequence which has an amino modified 5′end was used to conjugate to the activated carboxylic functional groups littered on the surface edges of the GO particles (Liu et al., 2010). Fifty microlitre of 100 μM of amino modified DNA target strand was added into the activated GO solution for 12 h under wrap with foil for immobilization. Excess EDC, Sulfo-NHS, GO particles and non-conjugated DNA target strands were removed by repeated centrifugation at 14,000 rpm. The precipitate which consisted of GO-DNA target was dissolved in a mixture of DMF and deionized nanopure H_2O at the ratio of 2:1 in volume. Characterization of both DNA conjugated nanoparticles consisting of Au NP-DNA and GO-DNA was done by measuring the shift in wavelength through spectrophotometry analysis and imaging utilizing HRTEM. Visual observation on the colour difference of the DNA conjugated nanoparticles was observed and captured through the use of a professional DSLR camera.

2.5. Selectivity and sensitivity testing

Detection of DNA hybridization through the use of the biosensor was done by preparing a plastic microfuge tube containing 50 μl of 5 μM complementary Au NP-DNA. Next, 50 μl of 1 μM complementary GO-DNA was added into the solution. Visual observation on the colour change was recorded and HRTEM was used for microscopic imaging. Spectrophotometry analysis was performed to detect any shift in wavelength. Experimentation on the first selectivity sample was done by addition of 50 μl of 1 μM non-complementary GO-DNA into a solution containing 50 μl of 5 μM Au NP-DNA. The second selectivity test involved pipetting 50 μl of 1 μM GO-DNA into a 50 μl solution containing 5 μM of non-conjugated, non-complementary DNA probe.

Sensitivity testing was performed by using serially diluted GO-DNA from the stock concentration of 1 μM. Each sample was sequentially diluted 50% from its previous sample concentration to provide 8 ranges of GO-DNA concentration at 0.5 μM, 0.25 μM, 0.125 μM, 62.5 nM, 31.25 nM, 15.62 nM, 7.81 nM and 3.91 nM. All GO-DNA samples were tested individually by adding equal amount into plastic microfuge tubes containing 50 μl Au NP-DNA solution at 5 μM. Both of the selectivity and sensitivity testings were characterized utilizing spectrophotometer analysis between the wavelengths of 215 nm and 700 nm. Visual observation was recorded with a DSLR camera and HRTEM imaging was performed to observe the overall shape and interaction between the DNA conjugated nanoparticles. The experiments were repeated 4 times to ensure reproducibility.

3. Result and discussion

3.1. Characterization of Au NP and Au NP-DNA

Based on visual inspection, the prepared Au NP was observed to be a pristine ruby red solution in Fig. 1AI. This indicates the nanoparticles were within the size range of 10–30 nm in diameter according to the Turkevich method in the preparation of monodisperse gold nanoparticles. Based on the spectrophotometry measurement in the wavelength scan, a peak was observed at 520 nm wavelength in Fig. 2A thus proving the production of 20 nm Au NP (Ding et al., 2012). Furthermore HRTEM images in Fig. 3A confirmed the size of the synthesized Au NP to be an average of 20 nm in diameter and its shape was observed to be spherical.

The conjugation of the 22 base pair long single stranded DNA probe based on the *inv*A gene of *S. enterica* to the 20 nm Au NP produced a pinkish-red solution which was observed through the naked eye (Fig. 1AIII). The relative reduction of the colour density in the Au NP-DNA probe solution when compared to the unconjugated Au NP solution was due to the lesser concentration of free nanoparticles required for conjugation with the available DNA probe. The spectrophotometer analysis of the Au NP-DNA gave a wavelength peak at 528 nm, which was a shift of 8 nm (Fig. 2A). This is due to the increase in size of the Au NP through conjugation to the DNA probe, thus confirming the attachment of the DNA probe to the nanoparticles. Similarly HRTEM images showed an increase in dispersion of the conjugated nanoparticles when compared to the Au NP in Fig. 3C. This was attributed to the single stranded DNA probe conjugated to the Au NP providing an extra negative charge thus strengthening the repulsion effect of the van der Waals forces, forcing the nanoparticles to be pushed further apart of similar particles (Zhao et al., 2008). A series of four repetitive wavelength analyses on the Au NP and Au NP-DNA gave a relative standard deviation of 4.5%.

3.2. Characterization of GO and GO-DNA

The synthesis of pristine GO solution through the improved phosphoric acid method produced a golden brown solution

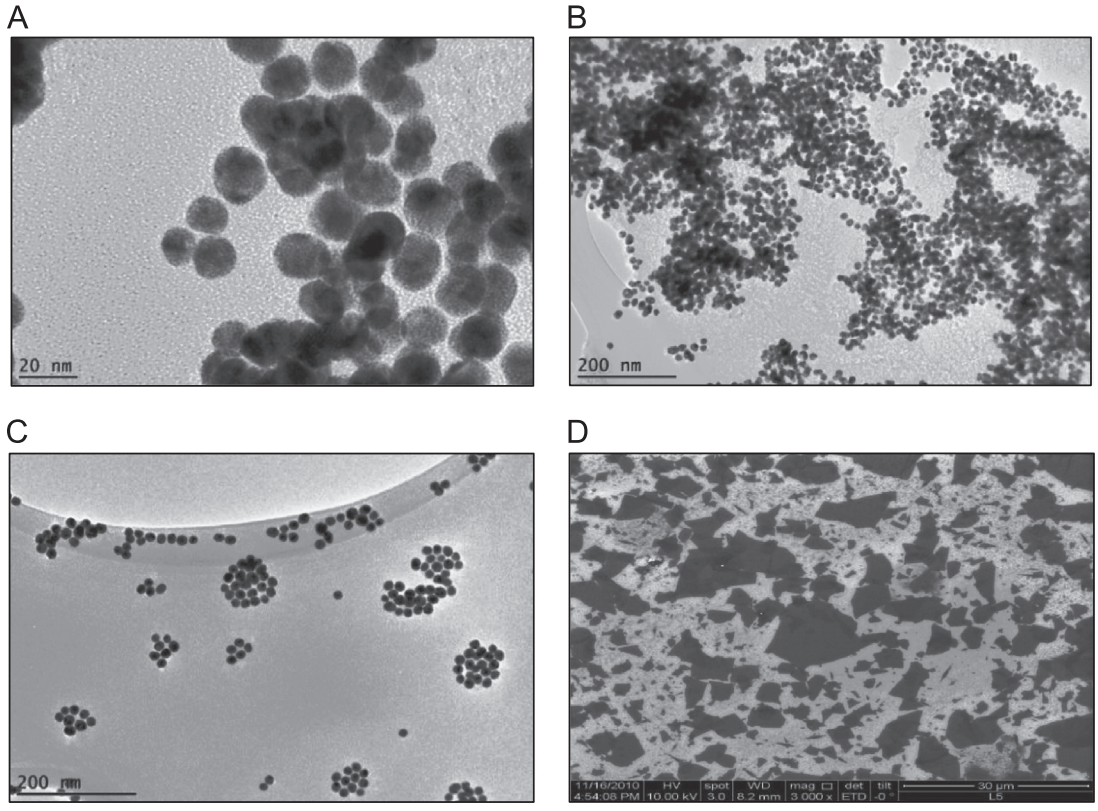

Fig. 3. HRTEM image of (A) Spherical 20 nm Au NP, (B) general visualization of slightly dispersed Au NP, (C) Au NP-DNA, and (D) FESEM image of pristine GO particles after sonication.

(Fig. 1AII). The spectrophotometry analysis gave a wavelength peak at 226 nm in Fig. 2B thus confirming the presences of pristine GO particles (Hu et al., 2012). The FESEM image in Fig. 3D shows the diameters of the horn sonicated GO ranged from 5 to 15 μm. This provided an ideal surface area for conjugation of the designated DNA target on a small surface area.

The conjugation of the single stranded DNA target to the GO particles produced a colour change from golden brown to a light brown solution as seen in Fig. 1IV. This change in colour was due to the low concentration level of GO particles which conjugated with the available DNA target. Spectrophotometry analysis of the GO-DNA gave two wavelength peaks at 230 nm and 245 nm but with the primary peak at 230 nm as seen in Fig. 2B. When compared to the wavelength peak of the unconjugated GO solution a shift of 4 nm was seen. This was due to the increase in the particle size within the solution because of the conjugation of the DNA target to the GO particles. The appearance of a second peak on the GO-DNA wavelength scan was due to the presence of DNA target within the solution. This gave a peak at around 245 nm which corresponds to the detection range of 240–260 nm for DNA strands (Mangathayaru et al., 2009). A series of four repetitive wavelength analyses on the GO and GO-DNA gave a relative standard deviation of 5%.

3.3. Analysis and functionalization principles of the biosensor

The basic principle and mechanism of the biosensor is illustrated in Scheme 1 which explains the step by step fabrication of the biosensor from the synthesis of the 20 nm Au NP and the GO particles to the detection of DNA hybridization. The biosensor is represented in two platforms consisting of Au NP-DNA and GO-DNA which appear pinkish-red in Fig. 1AIII and light brown solution in Fig. 1AIV. When both platforms are mixed together in equal quantity, DNA hybridization between both probe and target occurred instantaneously as seen in Fig. 1AV. This phenomenon of hybridization between the probe and target caused the initial colour of the biosensor solution within both platforms to change from pinkish-red to a purplish-blue solution with visible precipitation seen in Fig. 4A. The occurrence of precipitation is explained through the extreme aggregation caused between the Au NP-DNA and GO-DNA particles which have formed larger visible particles. This precipitation is due to the change in electrostatic charges between the hybridized Au NP-DNA and GO-DNA causing a reduction in the repulsion forces between both conjugated platforms. In conclusion qualitative results through visual observation gave a distinctive colour change for the biosensor observed from an initial pinkish-red to a purplish-blue solution.

Quantitative detection of the DNA hybridization was done utilizing spectrophotometry analysis to measure the shift in wavelength to justify the colour change observed when both platforms of Au NP-DNA and GO-DNA were mixed together. The wavelength peak of the biosensor (hybridized Au NP-DNA and GO-DNA) at 550 nm was compared to the initial wavelength peak of the Au NP-DNA solution at 528 nm, thus giving a shift of 22 nm as seen in Fig. 4B. This relatively wide shift in wavelength was due to the aggregation of both platforms which were brought about by the hybridization between the probe and target DNA strands. This shift also gives credence to the distinctive colour change of the biosensor solution observed in Fig. 4A. The HRTEM images in Fig. 1B showed the concentrated aggregation of Au NP-DNA on the GO-DNA particles without any dispersion in its surrounding. In Fig. 4C when both platforms of the DNA conjugated nanoparticles were mixed together, the secondary peak gave a 2 nm left shift with the wavelength peak at 243 nm. This shift was attributed to the aggregation of both platforms. The peak detection was mainly due to the presence of the recently hybridized probe and target DNA, where double stranded DNAs gives a slightly lower wavelength peak due the π-stacking of the bases within the double stranded DNA; this phenomenon is commonly known as hypocromicity. Thus from the observed results, it was concluded that DNA hybridization was successfully detected through visual observation and spectrophotometry analysis.

3.4. Specificity principle and analysis

The specificity of the biosensor system depended on the DNA probe being complementary to the DNA target. Thus the biosensor was tested with two types of non-complementary DNAs and one type of complementary DNA sample to determine its specificity and colour change ability as seen in Fig. 4B and C. The first specificity test was done with the addition of the Au NP-DNA solution with a non-complementary GO-DNA, this was to examine for the detection of a colour change through visual observation. Spectrophotometry analysis was conducted for the detection of any wavelength shift and change in colour due to unspecific aggregation of the nanoparticles. The wavelength peak of the spectrophotometer analysis utilising the non-complementary GO-DNA remained the same at 528 nm as seen in Fig. 4B. There

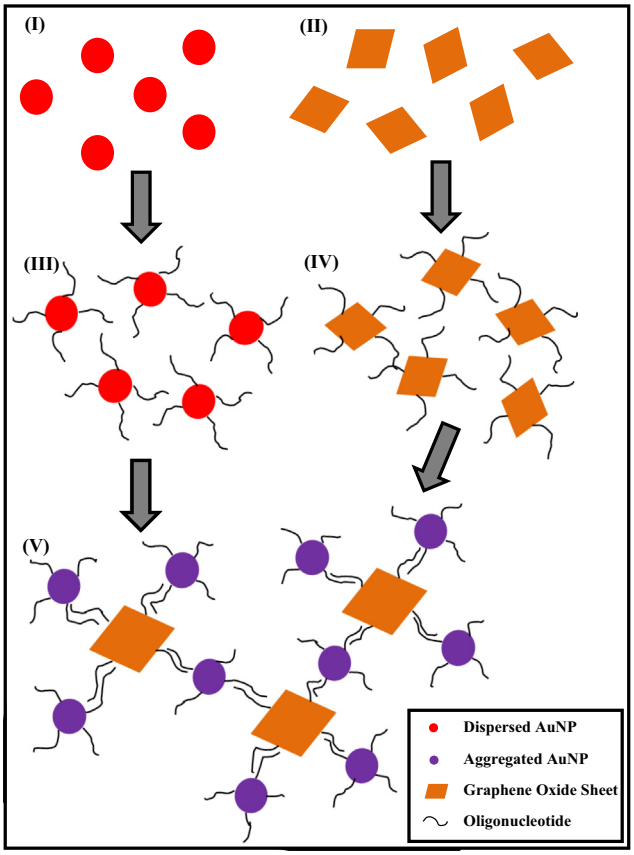

Scheme 1. Graphical representation of the biosensor in the detection of DNA hybridization. (I) Production of 20 nm Au NP through citrate reduction technique, (II) synthesis of 10 μm GO particles utilizing the improved phosphoric acid method, (III) conjugation of single strand DNA probe to Au NP through thiol linkages utilizing DTT, (IV) conjugation of single strand DNA target to GO particles through amide bonds with the addition of EDC and Sulpho-NHS, and (V) mixture of both platforms of the biosensor induces hybridization between the complimentary DNA probe and target, causing the aggregation of the Au NP-DNA onto the surface of the GO-DNA sheets producing an observable colour change from pinkish-red to light purplish.

was no colour change detected in the biosensor solution seen in Fig. 1AVI, for it remained a pinkish-red solution. The second specificity test was performed to observe if the GO-DNA platform could produce any colour change independent of the presence of Au NP which would invalidate the entire biosensor's effectiveness. This was done by introducing a non-complementary, unconjugated single stranded DNA into the GO-DNA solution. There was no observable change in the colour of the GO-DNA as seen in Fig. 1AVII. The final specificity test was performed using both complementary Au NP-DNA and GO-DNA. Both platforms of the DNA conjugated nanoparticles were mixed with equal amount and through visual observation in Fig. 4A a colour change was detected immediately from a pinkish-red to a purplish-blue solution. Spectrophotometry analysis indicated a right shift in the wavelength from 528 nm to 550 nm indicating aggregation between the Au NP-DNA and GO-DNA through DNA hybridization in Fig. 4B. A series of four repetitive wavelength analyses on the specificity experiments yielded a relative standard deviation of 8%. In conclusion, it shows that the biosensor was specific for the target DNA, providing the proof of concept using the DNA hybridization principle.

3.5. Sensitivity analysis of biosensor

Sensitivity testing was done to determine the detection limit of the biosensor in its ability to induce colour change and a wavelength shift in the event of DNA hybridization. The final limit in the colour change ability of the biosensor was detected with the addition of 7.81 nM of GO-DNA which induced a colour change from pinkish-red to a light purplish solution seen in Fig. 5AVIII. Spectrophotometry analysis in Fig. 5B indicates a right shift in the wavelength from 528 nm to 549 nm. The final biosensor sample of 3.91 nM of GO-DNA did not produce an observable colour change to indicate successful hybridization as can be seen in Fig. 5AIX and its subsequent spectrophotometry analysis in Fig. 5B indicates a wavelength peak at 514 nm, thus it was unable to detect DNA hybridization. This was due to the limited concentration of GO-DNA particles within the solution causing the inability of all the Au NP-DNA to aggregate on its surface thus most remained dispersed. These free Au NP-DNA are more negatively charged compared to its counterpart the hybridized Au NP-DNA on the GO-DNA particles. The free probes are single stranded DNAs as compared to the

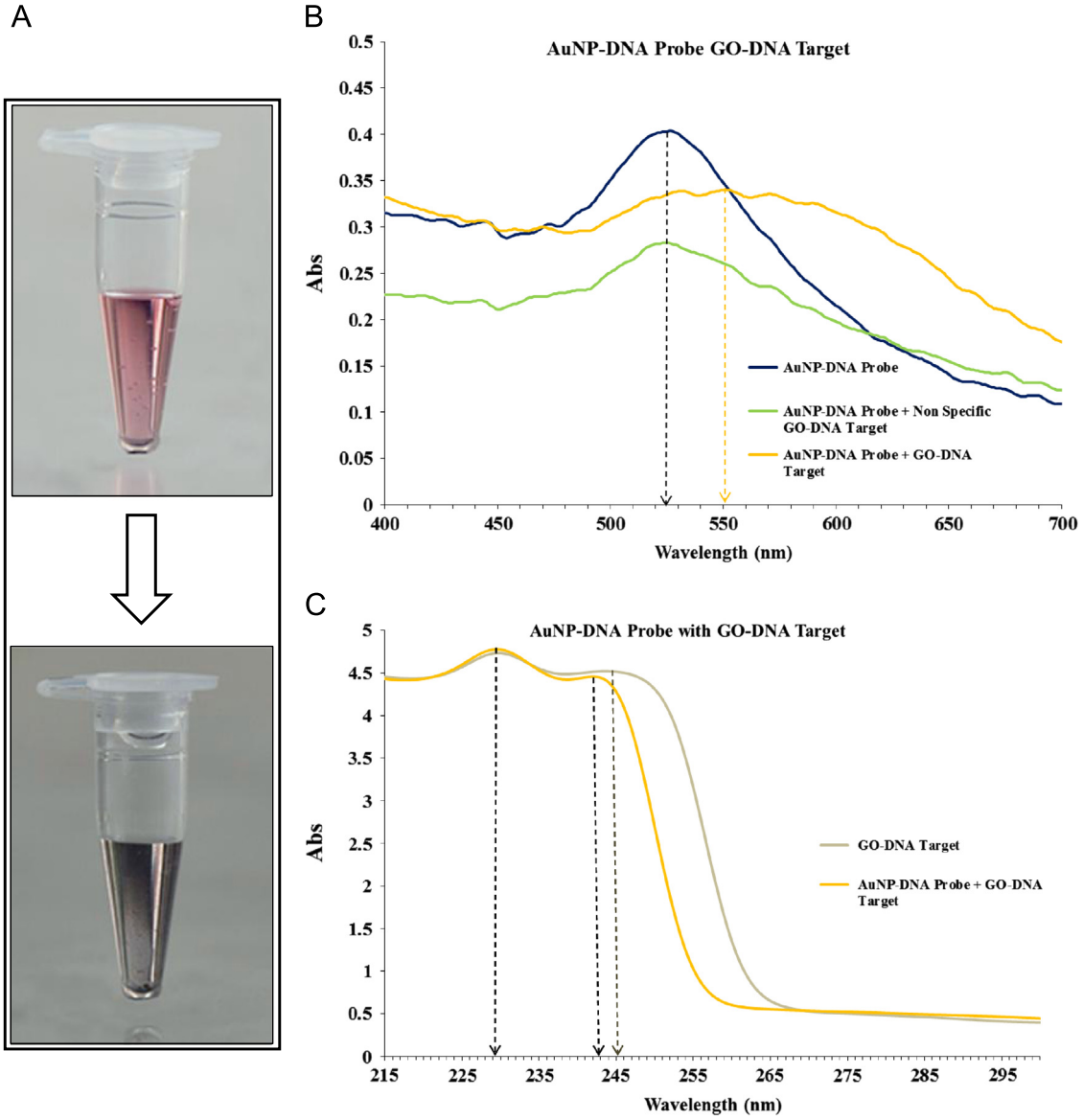

Fig. 4. (A) Colour change observed of the biosensor from (I) Pinkish red solution of Au NP-DNA before the addition of GO-DNA to (II) Purplish-blue solution of the biosensor after the addition of GO-DNA. Spectrophotometry analysis of the biosensor with negative control samples between (B) 400–700 nm and (C) 215–300 nm. (For interpretation of the references to color in this figure legend, the reader is referred to the web version of this article.)

hybridized double stranded DNA probes. This in effect further strengthens the van der Waals forces of repulsion between the DNA conjugated nanoparticles, forcing the dispersion to be greater apart, as indicated by the left shift in the spectrophotometer analysis. The highest level of detection indicated a shift from 528 nm to 602 nm at concentration of 62.5 nM of GO-DNA (Fig. 5AV). Such a huge shift in wavelength was detected for that particular concentration when compared to the other samples and this was most probably due to the ratio of GO-DNA particles being less in number compared to the Au NP-DNA, thus allowing the aggregation of all free Au NP-DNA onto the surface of the conjugated GO particles. Thus at concentration of 62.5 nM of GO-DNA, an equilibrium was achieved in the biosensor with 5 μM of Au NP-DNA where it was entirely hybridized, providing the optimum detection level for the biosensor. Subsequent use of lesser concentration of GO-DNA did not yield an equal or wider shift in wavelength because of the limited amount of free DNA conjugated GO particles present in the solution for the aggregation with the free Au NP-DNA. Furthermore the remaining un-hybridized dispersed AuNP-DNA within these solutions would cause the appearance of multiple smaller wavelength peaks on the spectrophotometry analysis as seen in Fig. 5B. A series of four repetitive spectrophotometry analyses on the sensitivity experimentation yielded a relative standard deviation of 8.3%. In summary the sensitivity of this particular DNA biosensor and its effectiveness is designed to function at an optimal condition when the target concentration is at approximately 60 nM with a minimum of target DNA limit at 8 nM.

3.6. Overview of dual nanoparticle biosensor

Although designs of colorimetric biosensors based on the dual nanoparticle have been reported, however our system differs in its mechanism. Most are based on the formation of a complex sandwich through aggregation of Au NP conjugated with single stranded DNA onto GO sheets (Li et al., 2013). The rationale behind the design is that double stranded DNA conjugated to Au NP is unable to aggregate onto the surface of the GO sheet. Thus detection is through negative detection while visual observation only shows a change in the intensity of the original colour of the solution. On the other hand, the system developed by us is of a new design in which it utilizes two distinct nanoparticles of Au NP and GO conjugated to respective DNA probe and target as separate platforms. The Au NP-DNA through hybridization is aggregated on the small surface area of the GO-DNA thus causing a shift in the surface plasmon resonance of the Au NP which in turn induces a visually distinct colour change. This label-free method of detection eliminates the use of enzyme, antibodies or florescence tagged particles which are commonly used in other DNA based sensors. Most developed biosensors utilizing the dual nanoparticle design are based on electrochemistry. The systems are based on depositing Au NP conjugated single stranded DNA onto GO sheets positioned above a three electrode system (Zhang and Jiang, 2012). It detects electrical current changes through signal amplification techniques using Adriamycin with the use of an electrochemical analyser with an optimal detection range from 1.0×10^{-8} to 1.0×10^{-13} mol dm^{-3}. In comparison, our goal was to develope

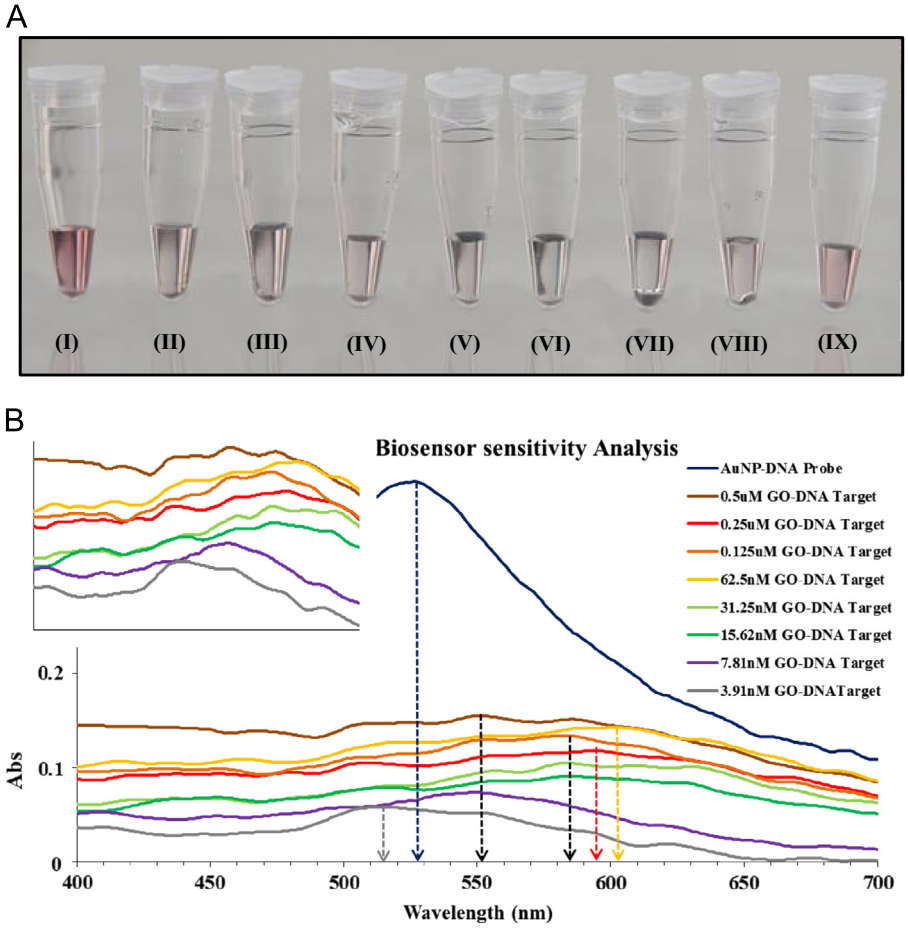

Fig. 5. (A) Visual observation of the colour change in the biosensor system in comparison with (I) Pinkish-red solution of Au NP-DNA. With the addition of GO-DNA to induce colour change at concentrations of (II) 0.5 μM, (III) 0.25 μM, (IV) 0.125 μM, (V) 62.5 nM, (VI) 31.25 nM, (VII) 15.62 nM, (VIII) 7.81 nM, and (IX) 3.91 nM. (B) Wavelength scans analysis of the biosensor system under differing concentration of GO-DNA used for the determination of the sensitivity effectiveness level. (For interpretation of the references to color in this figure legend, the reader is referred to the web version of this article.)

a relatively simple sensor so that it can be used in the field. Our system is based on direct visual detection without a need for complex detection equipment. Overall, with the use of the label free method and simplistic design in detection, the biosensor developed in this study provides a cost effective option when compared to other sensors in the market. The lowest sensitivity of the biosensor at 8 nM of DNA is on par and even better than other DNA hybridization sensors (Ma et al., 2012; Li et al., 2012). Similarly, the recently developed DNA hybridization sensors may have a detection range in the pico and femto molarity but they lack simplistic design, and detection rate (Xiang et al., 2012a; Gao et al., 2011).

4. Conclusion

In summary this work proves the success in visual detection of DNA hybridization through utilization of DNA conjugated dual nanoparticle platforms. Further improvements are being made to improve the system to detect unconjugated DNA sequences by utilizing a dual probe platforms thus expanding into genetic studies for microorganism identification.

Acknowledgement

We thank University of Malaya for the facilities and support. We would also like to thank Sanjay Kumar Ganasan of Sanjay Kawauchi Photography for his assistance in the visual observation of the biosensor system. This work was financially supported by the High Impact Research Grant of Ministry of Higher Education of Malaysia (UM.C/625/1/HIR/MOHE/05) and the Postgraduate Research Grant (PPP) (PV039-2011A) of University of Malaya.

References

Baptista, P., Doria, G., Henriques, D., Pereira, E., Franco, R., 2005. J. Biotechnol. 119 (2), 111–117.
Cao, Y.C., Jin, R., Thaxton, C.S., Mirkin, C.A., 2005. Talanta 67 (3), 449–455.
Ding, N., Zhao, H., Peng, W., He, Y., Zhou, Y., Yuan, L., Zhang, Y., 2012. Colloids Surf. A: Physicochem. Eng. Asp. 395 (0), 161–167.
Eum, N.-S., Kim, D.-E., Yeom, S.-H., Kang, B.-H., Kim, K.-J., Park, C.-S., Kang, S.-W., 2009. Biosystems 98 (1), 51–55.
Farré, M., Barceló, D., 2003. TrAC Trends Anal. Chem. 22 (5), 299–310.
Gao, Q., Zhang, W., Guo, Y., Qi, H., Zhang, C., 2011. Electrochem. Commun. 13 (4), 335–337.
Gao, W., Zhang, A., Chen, Y., Chen, Z., Chen, Y., Lu, F., Chen, Z., 2013. Biosens. Bioelectron. 49 (0), 139–145.
Hao, R.-Z., Song, H.-B., Zuo, G.-M., Yang, R.-F., Wei, H.-P., Wang, D.-B., Cui, Z.-Q., Zhang, Z., Cheng, Z.-X., Zhang, X.-E., 2011. Biosens. Bioelectron. 26 (8), 3398–3404.
He, Y.Q., Liu, S.P., Kong, L., Liu, Z.F., 2005. Spectrochim. Acta Part A: Mol. Biomol. Spectrosc. 61 (13–14), 2861–2866.
Hu, Y., Li, F., Han, D., Wu, T., Zhang, Q., Niu, L., Bao, Y., 2012. Anal. Chim. Acta 753 (0), 82–89.
Huang, X., El-Sayed, M.A., 2010. J. Adv. Res. 1 (1), 13–28.
Kim, E.Y., Stanton, J., Vega, R.A., Kunstman, K.J., Mirkin, C.A., Wolinsky, S.M., 2006. Nucleic Acids Res. 34 (7), e54.
Kleo, K., Kapp, A., Ascher, L., Lisdat, F., 2011. Anal. Biochem. 418 (2), 260–266.
Lalitha, P., Siti Suraiya, M.N., Lim, K.L., Lee, S.Y., Nur Haslindawaty, A.R., Chan, Y.Y., Ismail, A., Zainuddin, Z.F., Ravichandran, M., 2008. J. Microbiol. Methods 75 (1), 142–144.
Li, C., Yang, Y., Zhang, B., Chen, G., Wang, Z., Li, G., 2013. Part. Part. Syst. Charact., http://dx.doi.org/10.1002/ppsc.201300200.
Li, C.-Z., Karadeniz, H., Canavar, E., Erdem, A., 2012. Electrochim. Acta 82 (0), 137–142.
Lismont, M., Dreesen, L., 2012. Mater. Sci. Eng.: C 32 (6), 1437–1442.
Liu, F., Choi, J.Y., Seo, T.S., 2010. Biosens. Bioelectron. 25 (10), 2361–2365.
Loh, K.P., Bao, Q., Eda, G., Chhowalla, M., 2010. Nat. Chem. 2 (12), 1015–1024.
Lu, L.-P., Xu, L.-H., Kang, T.-F., Cheng, S.-Y., 2013. Chin. J. Anal. Chem. 41 (6), 805–810.
Ma, C., Wang, W., Li, Z., Cao, L., Wang, Q., 2012. Anal. Biochem. 429 (2), 99–102.
Mangathayaru, K., Umadevi, M., Reddy, C.U., 2009. J. Ethnopharmacol. 123 (1), 181–184.
Marcano, D.C., Kosynkin, D.V., Berlin, J.M., Sinitskii, A., Sun, Z., Slesarev, A., Alemany, L.B., Lu, W., Tour, J.M., 2010. ACS Nano 4 (8), 4806–4814.
Merkoçi, A., 2010. Biosens. Bioelectron. 26 (4), 1164–1177.
Nguyen, D.T., Kim, D.-J., Kim, K.-S., 2011. Micron 42 (3), 207–227.
Paddle, B.M., 1996. Biosens. Bioelectron. 11 (11), 1079–1113.
Qi, Y., Li, L., Li, B., 2009. Spectrochim. Acta Part A: Mol. Biomol. Spectrosc. 74 (1), 127–131.
Redshaw, N., Dickson, S.J., Ambrose, V., Horswell, J., 2007. Forensic Sci. Int. 172 (2–3), 106–111.
Sato, K., Hosokawa, K., Maeda, M., 2003. J. Am. Chem. Soc. 125 (27), 8102–8103.
Sharma, H., Mutharasan, R., 2013. Sens. Actuators, B 183 (0), 535–549.
Tawa, K., Yao, D., Knoll, W., 2005. Biosens. Bioelectron. 21 (2), 322–329.
Tolley, S.E., Wang, H.-k., Smith, R.S., Christensen, D.A., Herron, J.N., 2003. Anal. Biochem. 315 (2), 223–237.
Tothill, I.E., 2009. Semin. Cell Dev. Biol. 20 (1), 55–62.
Wang, J., 2002. Anal. Chim. Acta 469 (1), 63–71.
Wood, K.V., Gruber, M.G., 1996. Biosens. Bioelectron. 11 (3), 207–214.
Wu, H., Ji, X., Zhao, L., Yang, S., Xie, R., Yang, W., 2012. Colloids Surf. A: Physicochem. Eng. Asp. 415 (0), 174–179.
Wu, M., Kempaiah, R., Huang, P.-J.J., Maheshwari, V., Liu, J., 2011. Langmuir 27 (6), 2731–2738.
Xiang, X., Chen, L., Zhuang, Q., Ji, X., He, Z., 2012a. Biosens. Bioelectron. 32 (1), 43–49.
Xiang, X., Luo, M., Shi, L., Ji, X., He, Z., 2012b. Anal. Chim. Acta 751 (0), 155–160.
Yang, Y., Matsubara, S., Nogami, M., Shi, J., 2007. Mater. Sci. Eng.: B 140 (3), 172–176.
Zhan, Z., Ma, X., Cao, C., Sim, S.J., 2012. Biosens. Bioelectron. 32 (1), 127–132.
Zhang, Y., Jiang, W., 2012. Electrochim. Acta 71 (0), 239–245.
Zhao, W., Brook, M.A., Li, Y., 2008. Chembiochem.: Eur. J. Chem. Biol. 9 (15), 2363–2371.
Zhao, X.-H., Ma, Q.-J., Wu, X.-X., Zhu, X., 2012. Anal. Chim. Acta 727 (0), 67–70.
Zheng, B., Cheng, S., Liu, W., Lam, M.H.-W., Liang, H., 2012. Anal. Chim. Acta 741 (0), 106–113.
Zhou, J., Ralston, J., Sedev, R., Beattie, D.A., 2009. J. Colloid Interface Sci. 331 (2), 251–262.